

## Conserving Local Magnetic Helicity in Numerical Simulations.

YOSSEF ZENATI<sup>1</sup> AND ETHAN T. VISHNIAC<sup>1</sup>

<sup>1</sup>*Department of Physics and Astronomy, The Johns Hopkins University, Baltimore, MD 21218*

(Dated: April 2021)

### ABSTRACT

Magnetic helicity is robustly conserved in systems with large magnetic Reynolds numbers, including most systems of astrophysical interest. This plays a major role in suppressing the kinematic large scale dynamo and driving the large scale dynamo through the magnetic helicity flux. Numerical simulations of astrophysical systems typically lack sufficient resolution to enforce global magnetic helicity over several dynamical times. Errors in the internal distribution of magnetic helicity are equally serious and possibly larger. Here we propose an algorithm for enforcing strict local conservation of magnetic helicity in the Coulomb gauge in numerical simulations.

### 1. INTRODUCTION

Magnetic helicity is a conserved quantity in ideal MHD (Woltjer 1958) and one of the primary ways to quantify the complexity of a magnetic field. In a weakly nonideal turbulent system it is still almost conserved, in the sense that the turbulent cascade is ineffective at transferring it to resistive scales, even while the magnetic and kinetic energies are dissipated efficiently. Consequently Taylor (1974) offered the conjecture that a laboratory system would first relax to the minimum energy state with the same total magnetic helicity (see also Taylor (1986)). For example see Yamada (1999) for a review of the laboratory evidence accumulated in the following two decades. We note in particular Ji et al. (1996) which shows that the dynamical transport of magnetic helicity is an important part of this balance. The conservation of magnetic helicity should be even more robust in astrophysical systems where the microscopic resistivity is usually much less important on large eddy scales.

In addition to its importance in determining the relaxation of complex systems, magnetic helicity may play a role in the large scale dynamo process, a point that was first raised by Pouquet et al. (1976). The evolution of the large scale magnetic field  $\mathbf{B}_l$ , where the subscript denotes low pass filtering on the scale  $l$ , is given by

$$\partial_t \mathbf{B}_l = \nabla \times (\mathbf{v}_l \times \mathbf{B}_l) + \nabla \times \mathbf{e}_l, \quad (1)$$

where

$$\mathbf{e}_l \equiv (\mathbf{v} \times \mathbf{B})_l - \mathbf{v}_l \times \mathbf{B}_l. \quad (2)$$

In a turbulent medium  $\mathbf{e}_l$ , the electromotive force filtered on the scale  $l$ , is approximately the large scale average of the cross product of the turbulent velocity and magnetic fields. Pouquet et al. (1976) pointed out that  $\mathbf{e}_l$  has contributions from the eddy scale contributions to the averaged kinetic and

current helicities multiplied by  $\mathbf{B}_l$ , i.e. as a part of the  $\alpha$  effect in dynamo theory. Neither helicity is conserved in ideal MHD but in the Coulomb gauge the eddy scale current helicity,  $\mathbf{j} \cdot \mathbf{b}$ , is approximately  $k^2$  times the eddy scale magnetic helicity,  $\mathbf{a} \cdot \mathbf{b}$ , where  $k^2$  is the mean square wavenumber associated with the large scale eddies. While only the total magnetic helicity is conserved, the transfer of magnetic helicity between large and small scales depends on the parallel component of the electromotive force. This connection was exploited by Gruzinov & Diamond (1996) to show that a dynamo driven by the kinetic helicity saturates due to the local accumulation of magnetic helicity, and turns off long before the large scale field reaches equipartition with the turbulent energy density (" $\alpha$  suppression"). Apparently the conservation of magnetic helicity can have profound implications for the large scale dynamo.

Given the existence of large scale magnetic fields it seems safe to assume that there is some way to avoid the negative conclusion offered by Gruzinov & Diamond (1996). Possibly the kinematic dynamo operates, perhaps at a reduced efficiency, while the eddy scale magnetic helicity is ejected from the system (for a discussion of this idea see Brandenburg et al. (2009)). Alternatively the kinetic helicity may be irrelevant and a magnetic helicity flux, induced by rotation, creates local accumulations of eddy scale magnetic helicity which then drive a large scale dynamo as a side effect of being transferred to large scale fields (Vishniac & Cho 2001). Finally, it is possible that a large scale dynamo (LSD) could be produced through a combination of shear and fluctuating kinetic helicity (Vishniac & Brandenburg 1997; Mitra & Brandenburg 2012), although the relation between this mechanism and  $\alpha$  suppression has never been fully explored.

Regardless of which of these mechanisms dominate in real systems, we can see that accurate simulations of dynamos

require careful accounting of the distribution of magnetic helicity in a system. To model Taylor relaxation accurately one need only conserve the total magnetic helicity in a simulation box. To model dynamos, including  $\alpha$  suppression and the transport of magnetic helicity, one needs to extend this down to scales not much larger than individual eddy scales. Moreover, since the magnetic helicity is a quadratic quantity, the average magnetic helicity on domain scales can arise from correlations on eddy scales. The dissipation of this contribution to the magnetic helicity proceeds at the ohmic dissipation time at the large eddy scale (or a bit faster, see below). Numerical dissipation on this scale has to be slower than the large scale dynamo growth rate for an accurate large scale dynamo simulation. In practice, while this is a trivial threshold for real systems, it represents a substantial challenge for simulations. This is a particularly difficult issue for simulations of the magnetorotational instability, where the large scale eddy size is proportional to the strength of magnetic field. Worse is that the MRI operates primarily in the  $\hat{r}\hat{\phi}$  plane, and the vertical wave number in unstratified simulations tends to the dissipation scale, which guarantees that magnetic helicity will not be conserved for more than an eddy correlation time unless than magnetic Prandtl number is larger than one.

This raises the question of whether it might be useful to enforce magnetic helicity conservation in numerical simulations. In many cases it is possible to enforce conservation of an important conserved quantity by choosing an appropriate numerical algorithm, but magnetic helicity is nonlocal and no local numerical algorithm conserves it exactly. What price do we pay for adjusting the small scale magnetic field in real time to compensate for numerical errors? As a general rule, requiring strict conservation of any quantity will prioritize it above other conserved quantities. In particular, adjusting the magnetic field to conserve magnetic helicity will affect the stress energy tensor, and in particular the energy density. However, in a turbulent simulation the energy is continuously lost to the turbulent cascade, so energy conservation at small length scales is of secondary importance unless the energy input (or loss) is comparable to the turbulent energy dissipation rate. Any scheme that adjusts local magnetic field strengths will violate flux freezing, but that's already violated by transport in the turbulent cascade (Eyink et al. 2013). Lastly, if there is no turbulence, then there's almost no numerical loss of magnetic helicity and any scheme for correcting the field will have a negligible effect. In principle there seems to be no fundamental obstacle to implementing a correction scheme to enforce magnetic helicity conservation. Whether or not a particular scheme improves the accuracy of numerical simulations at an acceptable cost depends on the details of the algorithm. In this paper we will suggest an approach to en-

forcing magnetic helicity conservation and explore some of the constraints on its use.

## 2. DEFINING AN ALGORITHM

In a highly conducting fluid the magnetic field evolves as

$$\partial_t \mathbf{B} = \nabla \times (\mathbf{v} \times \mathbf{B} - \eta \mathbf{J}), \quad (3)$$

where the resistive term  $\eta \mathbf{J}$  is small. Numerical effects may or may not mimic a physical resistivity. We will assume here that they do, but note places where the difference might be important. Consequently the vector potential evolves as

$$\partial_t \mathbf{A} = \mathbf{v} \times \mathbf{B} - \eta \mathbf{J} - \nabla \phi, \quad (4)$$

where the electrostatic potential,  $\phi$  satisfies

$$\nabla^2 \phi = \nabla \cdot (\mathbf{v} \times \mathbf{B} - \eta \mathbf{J}), \quad (5)$$

in the coulomb gauge. This gauge choice has the advantage of enforcing a tight correlation between the small scale contribution to the current helicity,  $\mathbf{J} \cdot \mathbf{B}$ , and the small scale contribution to the magnetic helicity. The former is gauge invariant and plays an important role in dynamo theory. We note that other gauge choices have been used for computational convenience or because the magnetic helicity has some compelling interpretation in that gauge (for examples see (Hubbard & Brandenburg 2011; Candelaresi et al. 2011; Del Sordo et al. 2013)).

In this gauge the magnetic helicity flux is

$$\mathbf{J}_H \equiv \mathbf{A} \times (\mathbf{v} \times \mathbf{B} - \eta \mathbf{J} + \nabla \phi), \quad (6)$$

and the magnetic helicity,  $H$ , evolves as

$$\partial_t H = -\nabla \cdot \mathbf{J}_H - 2\eta \mathbf{J} \cdot \mathbf{B}. \quad (7)$$

When the resistivity is small its contribution to  $\mathbf{J}_H$  will be negligible, but its role in breaking magnetic helicity conservation can still be important. We can define the small scale contribution to the magnetic helicity as  $h_l \equiv H - \mathbf{A}_l \cdot \mathbf{B}_l$  so that the evolution equation is

$$\partial_t h_l = -\nabla \cdot \mathbf{J}_{Hl} - 2\eta (\mathbf{J} \cdot \mathbf{B})_l - 2\mathbf{B} \cdot \mathbf{e}_l. \quad (8)$$

The last term on the RHS of this equation describes the transfer of magnetic helicity between small and large scales. The coupling with  $h_l$  through this term takes the form  $V_A^2 k_{\parallel}^2 \tau_l h_l$ , where  $V_A$  is the Alfvén speed and  $\tau_l$  is the eddy turn over time on the scale  $l$ . Assuming critical balance (Goldreich & Sridhar 1997), or  $k_{\parallel} V_A \tau_l \sim 1$  this implies that magnetic helicity embedded in eddies at small scale is transferred to large scales in one eddy turn over time. The injection of magnetic helicity from large scales to small arises from the turbulent diffusion term in  $e_l$ , which is to say that it will be proportional to the turbulent transport coefficient  $v_l^2 \tau_l$ . Balancing

these effects implies that the magnetic helicity embedded in small scale structures will scale as  $v_l^2 \tau_l^2 \sim l^2$ , for all values of  $l$  in the turbulent cascade. In other words, we expect the current helicity,  $\sim l^{-2} h_l$  will be the same at all scales. This in turn implies that the dissipation of magnetic helicity will be enhanced by some logarithmic factor above the ohmic dissipation rate on the large eddy scale. Furthermore, simulations that use artificial forms of resistivity that depend on higher powers of the wavenumber will not damp magnetic helicity at appreciably slower rates. The reduced range of scales subject to dissipation will tend to accumulate extra power, and presumably magnetic helicity, due to the bottleneck effect.

Tracking magnetic helicity in a simulation requires calculating  $\nabla \cdot \mathbf{J}_H$ , which implies a knowledge  $\mathbf{A}$  and  $\phi$  everywhere. If the underlying code is pseudospectral, or is at least based on a regular grid, then this is straightforward (Squire & Bhattacharjee 2016). Otherwise the code has to be supplemented with Green's functions based routines that will calculate these quantities (Yousef et al. 2008; Singh & Jingade 2015).

The problem is that small numerical errors, due to discreteness effects, will produce an effective dissipation, leading to a magnetic field  $\mathbf{B}_{calc}$  which differs from the ideal result on small scales and whose associated magnetic helicity is not conserved (Bodo et al. 2017). We can calculate the ideal distribution of magnetic helicity in a simulation by calculating  $\nabla \cdot \mathbf{J}_H$  at every time step and advancing  $H$  accordingly.

Here we propose a rigorous procedure that will bring the magnetic helicity back into alignment with its expected value, while minimizing the size of the correction. We could write this as a straightforward Gaussian minimization problem by defining an action dependent on the mean square correction to the field, subject to constraints that ensure that the corrected field will have the correct magnetic helicity distribution and will satisfy the usual constraints on the magnetic field. This is

$$S \equiv \int [(1/2)(\delta\mathbf{B})^2 + \lambda(\mathbf{x})(H - \mathbf{A} \cdot \mathbf{B}) + \mu(\mathbf{x})\nabla \cdot \mathbf{B}]dV, \quad (9)$$

where  $H$  is the magnetic helicity distribution that we expect and  $A$  and  $B$  are the corrected values of the vector potential and magnetic field. The last term in the integral enforces usual zero divergence condition on the magnetic field. Without this term the corrected  $\mathbf{B}$  would no longer satisfy Maxwell's equations. It is not necessarily important to obtain the correct distribution of  $H$  on all scales. Just correcting it on scales comparable to, and larger than, the large scale eddy size would improve the accuracy of dynamo simulations.

Minimizing the change to the magnetic field is not the only choice. It's more convenient and more physically reasonable to minimize the change to the vector potential. The same change in the vector potential at small scales produces a larger change in  $B$ , so the net effect is that this choice puts

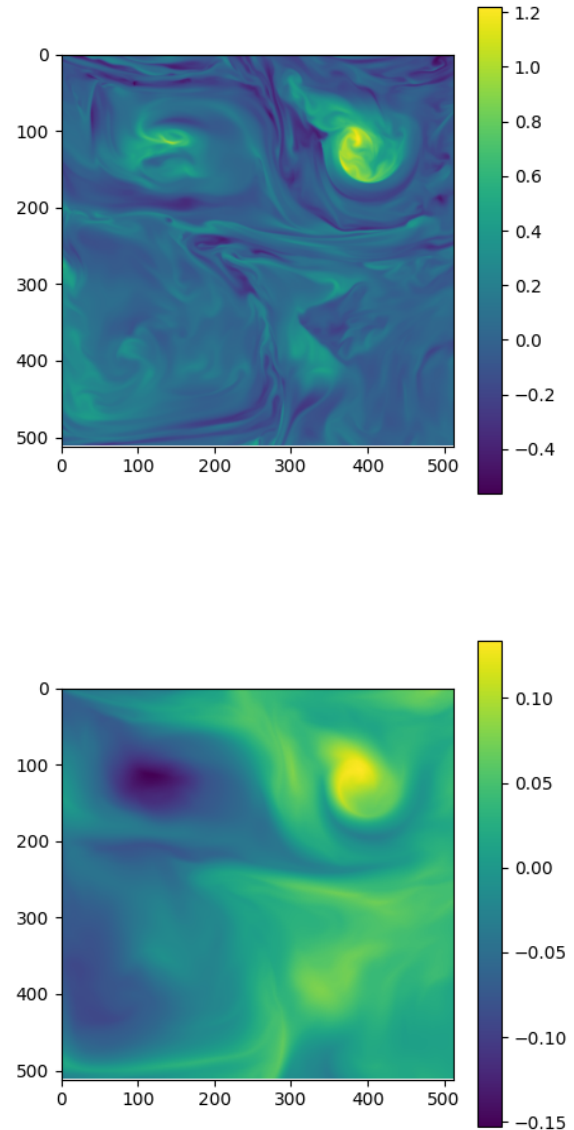


**Figure 1.** Upper: map of the magnetic field of 3D simulation taken from the TDB. This slice shown as a 512x512 size. Lower: map of the vector potential of the same slice 512x512 as the upper panel

more of the adjustment in the magnetic field at small scales. (This is not equivalent to correcting the magnetic helicity distribution at small scales. The magnetic field on small scales contributes to the large scale distribution of magnetic helicity.) This is a better choice, since we're trying to counteract the effects of inaccuracies at small scales. In addition, an algorithm which compensates for lost magnetic helicity by altering the large scale magnetic field runs the risk of driving a large scale dynamo by fiat. If we weight the algorithm by

$|\delta\mathbf{A}|^2$  then the action we choose to minimize is

$$S \equiv \int [(1/2)(\delta\mathbf{A})^2 + \lambda(\mathbf{x})(H - \mathbf{A} \cdot \mathbf{B}) - \mu(\mathbf{x})\nabla \cdot \mathbf{A}] dV. \quad (10)$$

The second Lagrangian constraint now fixes the gauge of  $\mathbf{A}$ , since the usual divergence free condition for  $\mathbf{B}$  is automatically satisfied. Integrating this by parts involves a surface term

$$\Delta S = \int [\lambda \mathbf{A} \times \delta\mathbf{A} - \mu \delta\mathbf{A}] \cdot d\mathbf{S}. \quad (11)$$

In a finite computational volume this gives us a pair of boundary conditions, that  $\lambda$  and  $\mu$  vanish nearly everywhere on the boundary, the only exception being places where  $\mathbf{A}$  is normal to the surface (for  $\lambda$ ). This guarantees that there is no nontrivial solution for  $\lambda$  unless the calculated distribution of magnetic helicity is nonzero somewhere. Here we will assume a periodic box and ignore this constraint. We obtain

$$\delta\mathbf{A} = 2\lambda\mathbf{B} + \nabla(\lambda) \times \mathbf{A} - \nabla\mu, \quad (12)$$

and

$$H = \mathbf{A} \cdot \mathbf{B}. \quad (13)$$

The second equation is just a restatement of our goal, that the field quantities should give the correct distribution of magnetic helicity. The first equation is not as simple as it appears, since the fields on the RHS are the corrected fields, not the calculated ones. The last term on the RHS arises from the Coulomb gauge and leads to

$$\nabla^2\mu = \nabla\lambda \cdot \mathbf{B} = \nabla \cdot (\lambda\mathbf{B}). \quad (14)$$

In order to make this problem more tractable, and to reduce the numerical cost of implementing a correction scheme, we will assume that  $\lambda$  is small and that we can therefore ignore the difference between the corrected and computed fields on the RHS of the first equation. This should be reasonable if the correction scheme is applied often enough. If we further assume that the correction to the magnetic helicity can be approximated to the same order, i.e. linear in  $\lambda$ , then we have a second order differential equation for  $\lambda(x)$  in the computational box. With some work, this can be shown to be

$$\begin{aligned} \Delta H &\equiv H - (\mathbf{A}_{calc} \cdot \mathbf{B}_{calc}) \\ &\approx \delta\mathbf{A} \cdot \mathbf{B} + \mathbf{A} \cdot (\nabla \times \delta\mathbf{A}) \\ &= 2\lambda B^2 + \mathbf{B} \cdot (\nabla\lambda \times \mathbf{A}) - \mathbf{B} \cdot \nabla\mu + 2\lambda \mathbf{J} \cdot \mathbf{A} \\ &\quad + 2\mathbf{A} \cdot (\nabla\lambda \times \mathbf{B}) + A_i A_j \partial_i \partial_j \lambda - \frac{1}{2} \nabla\lambda \cdot \nabla(A^2) - A^2 \nabla^2 \lambda \\ &= 2\lambda(B^2 + \mathbf{A} \cdot \mathbf{J}) - \nabla\lambda \cdot (\mathbf{A} \times \nabla \times \mathbf{A}) - \frac{1}{2} \nabla\lambda \cdot \nabla(A^2) \\ &\quad + (A_i A_j - A^2 \delta_{ij}) \partial_i \partial_j \lambda \\ &= 2(B^2 + \mathbf{A} \cdot \mathbf{J})\lambda + \partial_i ((A_i A_j - A^2 \delta_{ij}) \partial_j \lambda) - \mathbf{B} \cdot \nabla\mu \end{aligned} \quad (15)$$

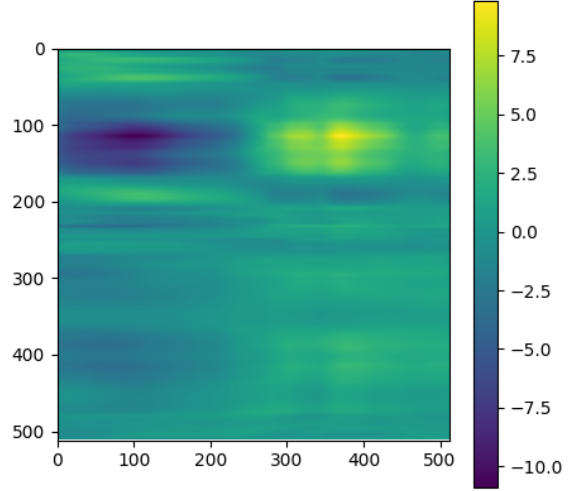


**Figure 2.** Map of the magnetic helicity of a slice 512x512 of 3D simulation following  $H = \mathbf{A} \cdot \mathbf{B}$ , you can see how the color map values are change

where we employ implicit summation over repeated indices. The last term can written as

$$\mathbf{B} \cdot \nabla\mu = \mathbf{B} \cdot \nabla \nabla^{-2} \nabla \cdot (\lambda\mathbf{B}). \quad (16)$$

The operator  $\nabla \nabla^{-2} \nabla$  is just  $\hat{k}\hat{k}$  in Fourier space. In real space it is an integral operator acting on everything to its right and can be written

$$\nabla \nabla^{-2} \nabla \cdot (\mathbf{F}) = \frac{\mathbf{F}}{3} + \int \frac{d^3 \mathbf{r}'}{4\pi r'^5} (3\mathbf{r}' \mathbf{r}' \cdot \mathbf{F}(\mathbf{r} + \mathbf{r}') - r'^2 \mathbf{F}(\mathbf{r} + \mathbf{r}')), \quad (17)$$

where  $\mathbf{F}$  is any differentiable vector field. As before, we are assuming that boundary conditions can be ignored. To linear order we obtain  $\lambda$  from

$$\begin{aligned} \Delta H &= 2(B^2 + \mathbf{A} \cdot \mathbf{J})\lambda + \partial_i ((A_i A_j - A^2 \delta_{ij}) \partial_j \lambda) \\ &\quad - \mathbf{B} \cdot \nabla \nabla^{-2} \nabla (\lambda\mathbf{B}), \end{aligned} \quad (18)$$

and use this in equation (12).

We need a general procedure for solving eq.(18). We can do this through iteration. If we split two of the coefficients on the RHS into varying and constant pieces defined by

$$C_0 \equiv \langle B^2 + \mathbf{J} \cdot \mathbf{A} \rangle = 2\langle B^2 \rangle, \quad (19)$$

$$C_1 \equiv B^2 + \mathbf{J} \cdot \mathbf{A} - C_0, \quad (20)$$

$$D_{0ij} \equiv \langle \delta_{ij} A^2 - A_i A_j \rangle, \quad (21)$$



**Figure 3.** Left: Log scale of the power spectrum of the original magnetic helicity and final magnetic helicity after modified by equation 18 as a function of modes. Right: Log scale of the power spectrum of the original vector potential A and the final vector potential after modified by equation 27 as a function of modes

and

$$D_{1ij} \equiv \delta_{ij}A^2 - A_iA_j - D_{0ij}, \quad (22)$$

then we can rewrite equation (18) as

$$\Delta H - 2C_1\lambda + \partial_i D_{1ij} \partial_j \lambda + \mathbf{B} \cdot \nabla (\nabla^{-2} \nabla \cdot (\lambda \mathbf{B})) = 2C_0\lambda - \partial_i D_{0ij} \partial_j \lambda. \quad (23)$$

The fourth term on the LHS of this equation resists any simple reduction since the operator  $\mathbf{B} \nabla^{-2} \mathbf{B}$  always depends on the wavenumber of  $\lambda(\mathbf{k})$ . In Fourier space the RHS of this equation is a simple multiplication by the positive definite coefficient

$$\lambda_{n+1}(\mathbf{k}) = \frac{1}{2C_0 + k_i k_j D_{0ij}} \left[ \Delta H(\mathbf{k}) + \left( -2C_1\lambda_n + \partial_i D_{1ij} \partial_j \lambda_n + \mathbf{B} \cdot \nabla (\nabla^{-2} \nabla \cdot (\lambda_n \mathbf{B})) \right) (\mathbf{k}) \right]. \quad (24)$$

The choice of  $\lambda_0$  is not dictated by this method. One possibility is to use  $\langle \Delta H \rangle / 2C_0$  as  $\lambda_0$  so that

$$\lambda_1 = \frac{1}{2C_0 + k_i k_j D_{0ij}} [\Delta H(\mathbf{k}) - C_1 \langle \Delta H \rangle / C_0]. \quad (25)$$

Alternatively we could choose

$$\lambda_0 = \frac{\Delta H}{2(C_0 + C_1)}. \quad (26)$$

The former captures the direct response to a helicity error at a wavenumber  $\mathbf{k}$  and a small part of the indirect response through the interaction with the spatial variation in the coefficient of  $\lambda$ . The latter captures the nonlinear part a bit better, but misses the dependence on gradients of  $\lambda$ .

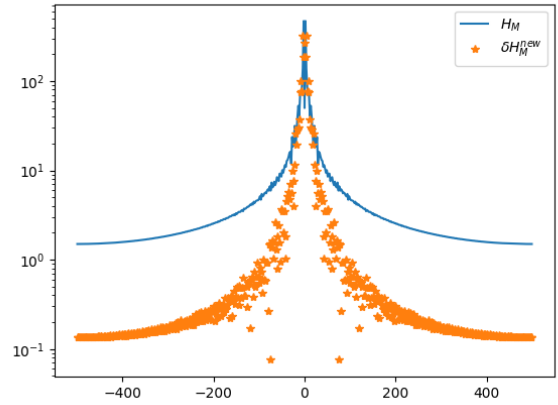


**Figure 4.** The magnetic helicity H (solid line) in the simulation which the algorithm run with smaller phase shift of the Fourier modes, easy to see  $\Delta H$  (dotted point) calculate by eq.23 is significantly smaller than H.

We can get a sense of how important the various contributions to  $\lambda$  are by considering two simple cases. In general we are concerned with correcting the distribution of magnetic helicity at scales significantly larger than an eddy scale, so we can assume that  $\Delta H(\mathbf{k})$  is nonzero only for wave numbers much smaller than the inverse of the large eddy scale. We expect the magnetic energy density will be largest at the large eddy scale, and the rms vector potential will be either largest at that scale or at the large scale magnetic field domain scale. In the former case we have  $C_0 \sim B_T^2 \sim D_{0ij} k_T^2$ , where  $k_T$  is the wave number of the large scale eddies. The fluctuating coefficients  $C_1$  and  $D_{1ij}$  will be functions of scale, but at the large eddy scale both are comparable to their nonfluctuating pieces. We see from eq.(23) that the contribution to



$\lambda$  from the large eddy scale will be comparable to that from the scales where  $\Delta H$  is nonzero. On smaller scales,  $l \ll l_T$  dominant term in  $C_1$  will be  $\mathbf{A} \cdot \mathbf{J}$ , which will be of order  $A_T A_l / l^2 \propto l^{-2/3}$  for the Goldreich-Sridhar model of turbulence. Consequently the contribution to  $\lambda$  from scales in the inertial cascade will decrease as  $l^{4/3}$

The magnetic domain scale vector potential can be larger than  $A_T$  even in early stages of the large scale dynamo. In this case the previous argument goes through in a slightly different form. Now the contribution to  $\lambda$  from the turbulent scale is reduced by a factor of  $A_T/A_0$  relative to the scale where  $\Delta H$  is nonzero. As before the contribution to  $\lambda$  falls off as  $l^{4/3}$  on smaller scales.

We conclude that solutions for  $\lambda$  need to be calculated to scales somewhat smaller than the large eddy scale in order to recover the desired distribution of magnetic helicity on magnetic domain scales.

After solving for  $\lambda$  to the required accuracy we correct the magnetic potential:

$$\delta \mathbf{A} = \nabla \times (\lambda \mathbf{A}) + \lambda \mathbf{B} - \nabla \nabla^{-2} \nabla \cdot (\lambda \mathbf{B}). \quad (27)$$

In phase space the last term does not have to be evaluated explicitly, rather the sum of the first two terms can simply be projected onto the plane perpendicular to  $\mathbf{k}$ . If the initial error in the magnetic helicity distribution is large then it may be necessary to iterate to allow for the nonlinear term  $(\nabla \times \delta \mathbf{A}) \cdot \delta \mathbf{A}$ .

If we neglect the gradient of  $\lambda$  and consider the correction to magnetic helicity, we find that

$$\Delta H \approx \mathbf{B} \cdot (2\lambda \mathbf{B}) + \mathbf{A} \cdot (\nabla \times 2\lambda \mathbf{B}) = 2\lambda (B^2 + \mathbf{A} \cdot \mathbf{J}). \quad (28)$$

The reconstituted magnetic helicity is not deposited strictly according to the energy density in the turbulent cascade, but on average it works out to the same thing as a function of scale. This implies that the power spectrum of the deposited magnetic helicity is much shallower than we would expect to find in a turbulent cascade. This is a consequence of eq. (27). There is some minimum scale, or maximum wavenumber, where the correction to the power spectrum is of order unity,  $k_{max} \lambda \sim 1$ . In order to avoid highly unphysical effects on the small scale turbulent spectrum we require that the dissipation scale wavenumber satisfy

$$1 > k_{diss} \lambda \sim \frac{k_{diss} \Delta H}{4 \langle B^2 \rangle}. \quad (29)$$

We can use this to set a limit on the cadence of corrections since we need

$$\Delta H < 4 \langle B^2 \rangle l_{diss}. \quad (30)$$

### 3. DISCUSSION AND CONCLUSIONS

In this study we have constructed an algorithm for correcting errors in the magnetic helicity distribution in numerical

simulations. The magnetic helicity is an important topological quantity that constrains large scale relaxation of magnetized systems and plays an important role in large scale dynamos. Numerical simulations that include turbulence frequently show a loss in global magnetic helicity. Tracking errors in its distribution within simulation volumes is more difficult, but likely to be a source of error. While there is no unique way to restore lost information, the algorithm explored here has some attractive features, including the ability to embed the lost helicity to roughly the same scales where numerical errors eliminated it.

We have examined the cleaning algorithm for magnetic helicity in the JHU 1024<sup>3</sup> MHD turbulence simulation. The algorithm restored the large scale distribution of magnetic helicity after it was distorted by randomly altering the phases of Fourier components of the magnetic field. The iterative procedure for constructing the solution converged, despite a lack of a formal proof of convergence. As expected the algorithm does increase the amount of very small scale power in the turbulent cascade, a result which needs to be considered in setting the cadence of correction in a simulation. We also note that while magnetic helicity is robustly conserved with any gauge choice our work is aimed specifically at enforcing conservation in the Coulomb gauge. We justify this choice by pointing to the close correlation between the magnetic helicity in this gauge and the current helicity, which appears in analytic theories of the large scale dynamo (and is not gauge dependent).

One complication is that we have not formally demonstrated that our procedure for deriving  $\lambda$  will always converge. We have shown, as a practical matter, that it converges in our test case, a simulation of homogeneous isotropic magnetized turbulence. This is a sufficiently robust test that it is plausible that it will always converge. However, we note that the fluctuating parts of the coefficients in the second order equation for  $\lambda$ , eq. (18), will be roughly as large as the constant parts. Moreover, the gauge constraint term will typically be of order  $\lambda B^2$ , i.e. the same order as the first RHS term. We have already seen that in real space this term is the sum of  $\lambda B^2/3$  plus a local quadrupole contribution which we can reasonably expect to be smaller. We can compare it to the first RHS term, whose average value is  $4B^2 \lambda$ . We see that the gauge constraint term will be smaller by an order of magnitude than the other terms on the RHS.

The difficulty of enforcing strict conservation of magnetic helicity in MHD simulations is a major obstacle in performing realistic simulations of large scale dynamo processes in astrophysical objects. This is particularly true for the magnetorotational instability, where the large scale eddy size can vary dramatically over time. More generally, magnetic helicity conservation may play a key role in the shear-current effect (Squire & Bhattacharjee 2016). Moreover, for

small-scale MHD fluctuations this effect may define the off-diagonal turbulent diffusivity  $\eta_{xy}$  (Singh & Jingade 2015; Squire & Bhattacharjee 2016; Singh & Jingade 2015; Jingade & Singh 2021; Dewar et al. 2020). As a result this could be the crucial bound of for MHD instabilities. Our results show that a viable correction scheme exists can be used to produce a realistic magnetic helicity distribution. In future work we will include this cleaning algorithm in a stratified periodic shearing box simulation (see, for example Davis et al.

(2010)) to follow the flow of magnetic helicity and its effect on the magnetorotational instability drive dynamo.

#### 4. ACKNOWLEDGEMENTS

This work makes used of Johns Hopkins Turbulence Database The authors wish to recognize and acknowledge helpful discussions with Amir Jafari and Greg Eyink. ETV thanks the AAS for supporting his research. YZ thank Mor Rozner for stimulating discussions. YZ thanks the CHE Israelis Excellence Fellowship for Postdoctoral for supporting his research.

## APPENDIX

### A. EXAMPLE

#### A.1. Example- calculation of first $\lambda$

Here we illustrate the method by applying it to a situation where the magnetic field is primarily described by a single large scale mode and consider how the this correction method copes with a small  $\Delta H$  which is small and also described by a single wave number. In this case,

$$\mathbf{A} = A_x \sin(kz)\hat{x} + A_y \sin(kz + \phi)\hat{y}, \quad (\text{A1})$$

so

$$\mathbf{B} = -kA_y \cos(kz + \phi)\hat{x} + kA_x \cos(kz)\hat{y}. \quad (\text{A2})$$

The magnetic helicity is  $kA_x A_y \sin(\phi)$ . The coefficients for equation (23) are

$$\begin{aligned} C_0 &= 2k^2(A_x^2 + A_y^2), \\ C_1 &= 0, \\ D_{0ij} &= \frac{A_y^2}{2}\hat{x}\hat{x} + \frac{A_x^2}{2}\hat{y}\hat{y} - \frac{A_x A_y}{2}\cos(\phi)(\hat{x}\hat{y} + \hat{y}\hat{x}) + \frac{A_x^2 + A_y^2}{2}\hat{z}\hat{z} \\ D_{1ij} &= -\frac{A_y^2}{2}\cos(2kz + 2\phi)\hat{x}\hat{x} - \frac{A_x^2}{2}\cos(2kz)\hat{y}\hat{y} + \frac{A_x A_y}{2}\cos(2kz + \phi)(\hat{x}\hat{y} + \hat{y}\hat{x}). \end{aligned} \quad (\text{A3})$$

In the simplest case, we can consider a constant perturbation to the helicity, i.e. some small  $\Delta H$  uniform over space. In this case

$$\lambda = \lambda_0 = \frac{\Delta H}{4k^2(A_x^2 + A_y^2)}. \quad (\text{A4})$$

Since  $\lambda_0$  is constant, all its spatial derivatives are zero and equation (23) gives a sequence of identical  $\lambda_n$ .

#### A.2. Example- sensitivity of the helicity distribution

In Fig. 5 and 6 we plot the solution of the algorithm we investigate in this study. We solve the basic solution in Fourier space with different shifted  $\delta H$ , this sensitivity illustrate the final solution we expected from whole 3D simulation we run.

## REFERENCES

- Bodo, G., Cattaneo, F., Mignone, A., & Rossi, P. 2017, ApJ, 843, 86, doi: [10.3847/1538-4357/aa7680](https://doi.org/10.3847/1538-4357/aa7680)
- Brandenburg, A., Candelaresi, S., & Chatterjee, P. 2009, MNRAS, 398, 1414, doi: [10.1111/j.1365-2966.2009.15188.x](https://doi.org/10.1111/j.1365-2966.2009.15188.x)
- Candelaresi, S., Hubbard, A., Brandenburg, A., & Mitra, D. 2011, Physics of Plasmas, 18, 012903, doi: [10.1063/1.3533656](https://doi.org/10.1063/1.3533656)
- Davis, S. W., Stone, J. M., & Pessah, M. E. 2010, ApJ, 713, 52, doi: [10.1088/0004-637X/713/1/52](https://doi.org/10.1088/0004-637X/713/1/52)

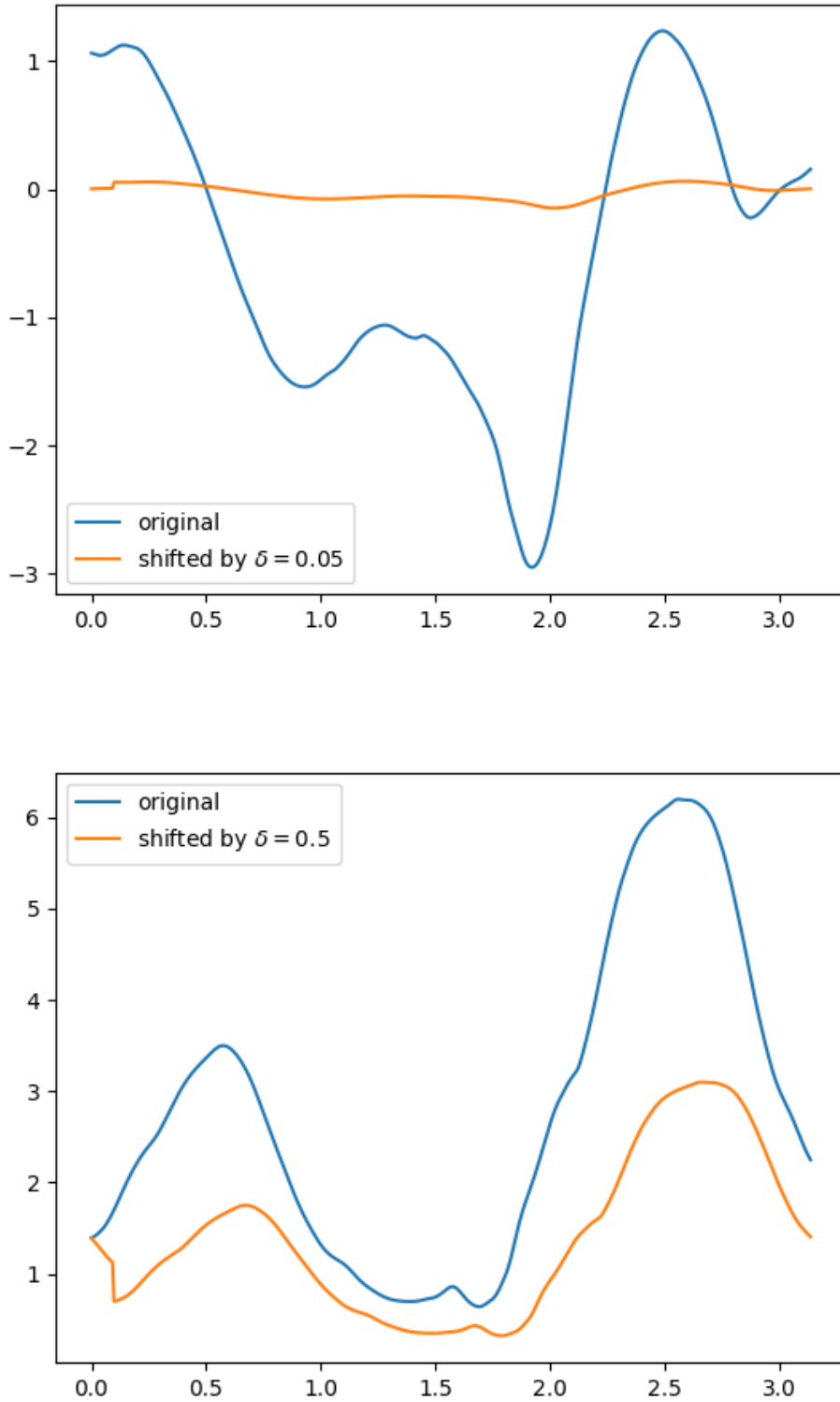


**Figure 5.** A mimic solution of the algorithm as a function of shift modes in Fourier space ( $\delta$ ) with small wave-numbers. The blue curve is the magnetic helicity  $H = \mathbf{A} \cdot \mathbf{B}$  and the orange curve are the new helicity in Fourier space as a function of  $\delta$ . The upper and lower panel are the same boundary conditions with free  $\delta$  parameters [0.05,0.5] respectively.



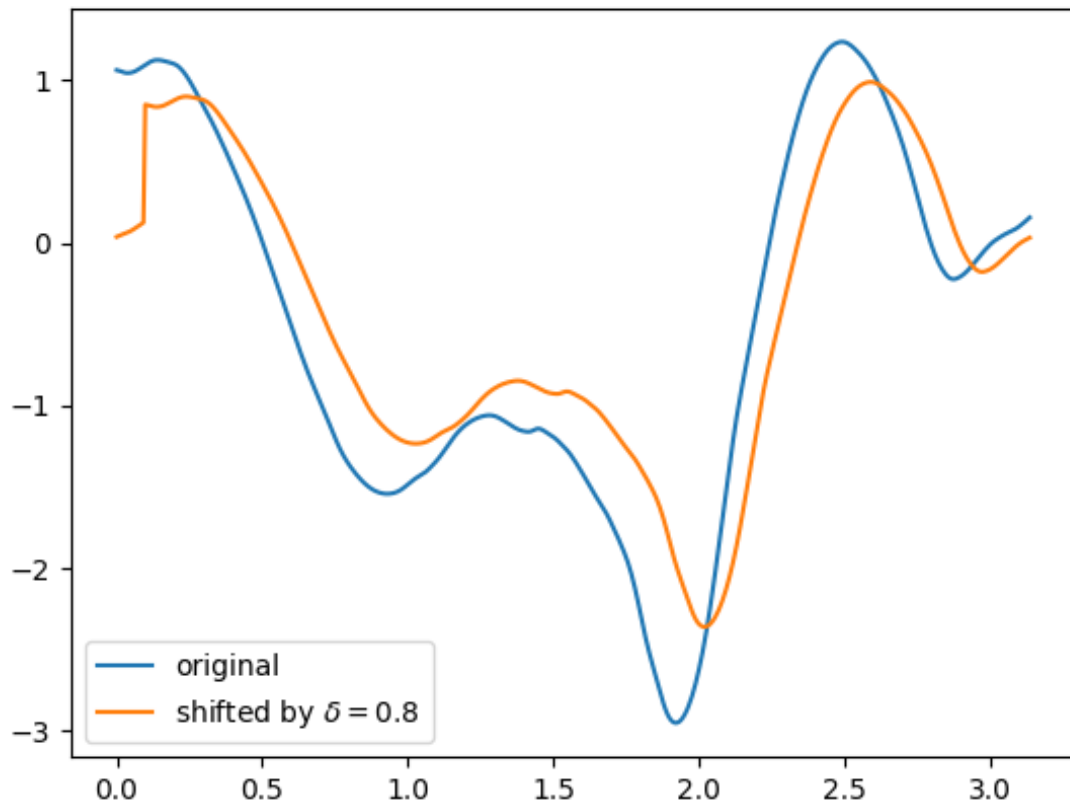


**Figure 6.** The same as fig. 5 with larger  $\delta = 0.8$ .

- Del Sordo, F., Guerrero, G., & Brandenburg, A. 2013, MNRAS, 429, 1686, doi: [10.1093/mnras/sts398](https://doi.org/10.1093/mnras/sts398)
- Dewar, R. L., Burby, J. W., Qu, Z. S., Sato, N., & Hole, M. J. 2020, Physics of Plasmas, 27, 062504, doi: [10.1063/5.0005740](https://doi.org/10.1063/5.0005740)
- Eyink, G., Vishniac, E., Lalescu, C., et al. 2013, Nature, 497, 466, doi: [10.1038/nature12128](https://doi.org/10.1038/nature12128)
- Goldreich, P., & Sridhar, S. 1997, ApJ, 485, 680, doi: [10.1086/304442](https://doi.org/10.1086/304442)
- Gruzinov, A. V., & Diamond, P. H. 1996, Physics of Plasmas, 3, 1853, doi: [10.1063/1.871981](https://doi.org/10.1063/1.871981)
- Hubbard, A., & Brandenburg, A. 2011, ApJ, 727, 11, doi: [10.1088/0004-637X/727/1/11](https://doi.org/10.1088/0004-637X/727/1/11)
- Ji, H., Prager, S. C., Almagri, A. F., et al. 1996, Physics of Plasmas, 3, 1935, doi: [10.1063/1.871989](https://doi.org/10.1063/1.871989)
- Jingade, N., & Singh, N. K. 2021, arXiv e-prints, arXiv:2103.12599. <https://arxiv.org/abs/2103.12599>
- Mitra, D., & Brandenburg, A. 2012, MNRAS, 420, 2170, doi: [10.1111/j.1365-2966.2011.20190.x](https://doi.org/10.1111/j.1365-2966.2011.20190.x)
- Pouquet, A., Frisch, U., & Leorat, J. 1976, Journal of Fluid Mechanics, 77, 321, doi: [10.1017/S0022112076002140](https://doi.org/10.1017/S0022112076002140)
- Singh, N. K., & Jingade, N. 2015, ApJ, 806, 118, doi: [10.1088/0004-637X/806/1/118](https://doi.org/10.1088/0004-637X/806/1/118)
- Squire, J., & Bhattacharjee, A. 2016, Journal of Plasma Physics, 82, 535820201, doi: [10.1017/S0022377816000258](https://doi.org/10.1017/S0022377816000258)
- Taylor, J. B. 1974, PhRvL, 33, 1139, doi: [10.1103/PhysRevLett.33.1139](https://doi.org/10.1103/PhysRevLett.33.1139)
- . 1986, Reviews of Modern Physics, 58, 741, doi: [10.1103/RevModPhys.58.741](https://doi.org/10.1103/RevModPhys.58.741)
- Vishniac, E. T., & Brandenburg, A. 1997, ApJ, 475, 263, doi: [10.1086/303504](https://doi.org/10.1086/303504)
- Vishniac, E. T., & Cho, J. 2001, ApJ, 550, 752, doi: [10.1086/319817](https://doi.org/10.1086/319817)
- Woltjer, L. 1958, Proceedings of the National Academy of Science, 44, 489, doi: [10.1073/pnas.44.6.489](https://doi.org/10.1073/pnas.44.6.489)
- Yamada, M. 1999, Washington DC American Geophysical Union Geophysical Monograph Series, 111, 129, doi: [10.1029/GM1111p0129](https://doi.org/10.1029/GM1111p0129)
- Yousef, T. A., Heinemann, T., Rincon, F., et al. 2008, Astronomische Nachrichten, 329, 737, doi: [10.1002/asna.200811018](https://doi.org/10.1002/asna.200811018)